

Simulations of Material Damage and high Energy Fluxes to ITER Divertor and First Wall during Transients and Runaway Electron Loads

B. Bazylev 1), I. Landman 1), S. Pestchanyi 1), Yu. Igitkhanov 1), A. Loarte 2), R. Pitts 2), M. Lehnen 3), V. Safronov 4), V. Podkovyrov 4), N. Klimov 4), I. Garkusha 5), W. Makhlay 5)

1) Karlsruhe Institute of Technology, IHM, P.O. Box 3640, 76021 Karlsruhe, Germany

2) ITER Organization, Route de Vinon sur Verdon, 13115 Saint Paul Lez Durance, France

3) Association Euratom- Institut für Plasmaphysik Jülich, D-5245 Jülich, Germany

4) SRC RF TRINITI, Troitsk, 142190, Moscow Region, Russia

5) Institute of Plasma Physics of the National Science Centre, Kharkov Institute of Physics and Technology, 61108 Kharkov, Ukraine

E-mail of main author: boris.bazylev@ihm.fzk.de

Abstract. In ITER the CFC and tungsten macrobrush armour as the PFC for the divertor and the dome, and beryllium macrobrushes for the first wall (FW) are foreseen. The fluid motion in a thin molten layer of W and Be during powerful transients may produce a splashing and thus dust emission by solidified droplets. The expected erosion of the ITER PFCs is estimated by numerical simulations validated against erosion experiments at the plasma gun facilities QSPA-T, MK-200UG and QSPA-Kh50. The measured material erosion was used to validate the codes MEMOS and PEGASUS that were then applied to model the erosion of ITER PFCs under the anticipated transient loads. The results of experiments carried out at QSPA-T allowed to validate MEMOS model for the melt splashing based on Kelvin-Helmholtz- and Rayleigh-Taylor instabilities. The crack formation at W surface was modeled using the code PEGASUS and validated against the experiments carried out at QSPA-Kh50. The models were applied for simulations of the PFCs damage under expected ITER-like scenarios. Numerical simulations under runaway electron impact with the codes ENDEP and MEMOS (validated against JET experiments) performed for expected ITER like heat loads demonstrated importance of evaporation from the armour surface which significantly decreases the melt sickness. The paper describes also recent simulations with the tokamak code TOKES. The numerical results on the radiation energy distribution over the vessel surface during for the massive gas injection in ITER and TOKES validation against DIII-D experiments are presented.

1. Introduction

The anticipated regime of the tokamak ITER is the H-mode [1] in which the repetitive outbreaks of the edge-localized mode (ELM) produce plasma fluxes which determine the erosion rate and the lifetime of PFCs [2]. The disruptions can also reduce the PFC lifetime [3], despite of mitigation measures such as the massive gas injection (MGI), in particular because of high heat fluxes by runaway electrons and radiation flush. The lost plasma dumped mainly into the scrape-off layer (SOL) and the impurity radiation produce surface erosion by sputtering, melting, cracking and vaporization. On the basis of scaling from present experiments [2,3], due to a high thermal energy of ITER core DT plasma (more than 0.3 GJ) the expected transient heat fluxes on the PFCs are as follows. I) Divertor target: ELM (type I) flux $0.5 - 4 \text{ MJ/m}^2$ on the timescale 0.3-0.6 ms. Thermal quench flux $2 - 13 \text{ MJ/m}^2$ in 1-3 ms. II) Main wall: ELM flux $0.5 - 2 \text{ MJ/m}^2$ in 0.3-0.6 ms. Thermal quench flux $0.5 - 5 \text{ MJ/m}^2$ in 1-3 ms. Mitigated disruption radiative flux $0.1 - 2 \text{ MJ/m}^2$ in 2-5 ms. The runaway flux more than 10 MJ/m^2 on timescale 10-100 ms. Furthermore, the following contamination of core plasma by eroded atoms can drastically deteriorate the confinement.

In ITER the CFC and tungsten macrobrush armour as the PFC for the divertor and the dome, and beryllium macrobrushes for the first wall (FW) are foreseen. After the transients, surface melting and surface cracking are seen as the main erosion mechanisms. The fluid motion in a thin molten layer of W and Be may produce a splashing and thus dust emission by solidified

droplets. An intense crack formation was observed for the CFC and W targets at large heat fluxes.

The expected erosion of ITER PFCs and the plasma heat fluxes under the transient loads can be adequately estimated by numerical simulations using the codes validated by experimental data. Within a collaboration established in fusion programme of EU, RF and the Ukraine, CFC and W macrobrush targets manufactured for the ITER divertor have been exposed to the ITER ELM-like and disruption-like loads at the plasma gun facilities QSPA-T, MK-200UG and QSPA-Kh50 [4,5]. The measured material erosion has been used to validate the modelling codes MEMOS and PEGASUS that have been then applied to model the erosion of ITER PFCs under the anticipated transient loads.

The code MEMOS describes fluid motion on molten surfaces taking into account such material properties as the surface tension and the viscosity. In the code the plasma pressure variations along the surface, as well as the gradient of surface tension and the $\mathbf{J} \times \mathbf{B}$ force caused by the currents crossing the melt layer immersed in strong magnetic field as well as by the eddy current generated due to the poloidal field evolution, produce the melt acceleration. The melt motion can result in melt splashing generated by growth of surface waves due to the Kelvin-Helmholtz- and Rayleigh-Taylor instabilities. The recent MEMOS simulations [6,7] performed for Be targets demonstrated that the $\mathbf{J} \times \mathbf{B}$ force generates a violent melt motion and thus becomes the most dangerous mechanism of the melt splashing for the first wall. During a mitigated disruption, the radiation and runaway electron loads at the armour can also produce the damage such as the surface melting up to the thickness of hundreds microns. Numerical simulations under radiation and runaway electron impact with code MEMOS were performed for expected ITER like heat loads [8,9]. Importance of evaporation from the armour surface for runaway heat loads which significantly decreases the melt sickness was demonstrated [9]. The W macrobrush structure can effectively prevent gross melt layer displacement thus decreasing the erosion both for single and multiple transient loads [8].

The results of experiments carried out at QSPA-T allowed validate the KIT model for the melt splashing based on Kelvin-Helmholtz- and Rayleigh-Taylor instabilities. Rather good agreement in size distribution of ejected droplet and the velocities of droplet emission was obtained [10,11]

The code PEGASUS describes such processes in W and CFC as crack formation, dust production and thermal conductivity deterioration [12]. A reasonable agreement with the experimental data of QSPA-Kh50 facility [13] has been obtained [12]. The simulations reproduce main morphology features of eroded surface of tungsten surface and the sizes of debris, as well as the measured erosion rate [13].

The paper will also describe the integrated tokamak simulations developed in KIT for transient loads with account for the following plasma contamination. The tokamak geometry MHD code TOKES has been developed. In this code the fluids are ionized plasma species from hydrogen isotopes to tungsten of different charge states and bound electron excitation states. The detailed species description allowed full corona model for the ionization equilibrium and thus adequate radiation losses from the confinement region [14,15]. The influx into the confinement region and the SOL of the neutral atoms emitted by the walls is taken into account.

Latest modelling results of TOKES on the radiation energy distribution over the vessel surface during MGI in ITER will be presented. In the simulations the injected noble gas gets ionized in the plasma, and then the ions dump into the scrape-off layer (SOL) and impact on the target. The contamination of core plasma results in fast loss of plasma energy by radiation. For MGI modelling TOKES was upgraded with toroidally symmetric two-dimensional

plasma model [16]. The new model is compared with the tokamak DIII-D and predictive simulations for ITER performed, with the conclusion that after the radiation flush in front of jet entry the wall temperature can exceed the beryllium melting point.

2. Modelling of runaway electron beams impact for JET and ITER

2.1 Simulations of runaway electrons impact for JET experiments.

Simulations of impact of the runaway electrons generated during MGI experiments at JET at the CFC first wall are used for the validation codes ENDEP and MEMOS. Volumetric energy deposition functions are calculated using the Monte Carlo code ENDEP and the code MEMOS is applied for the calculations of temperature distributions inside the CFC target with taking into account temperature-dependent thermo-physical properties of the CFC and peculiarities of upper wall construction [9,17].

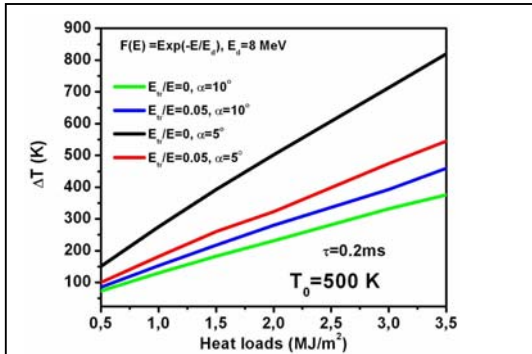


Fig. 1. Dependence of surface temperature rise at the center of RE impact spot as a function of heat loads for different scenarios of RE impact.

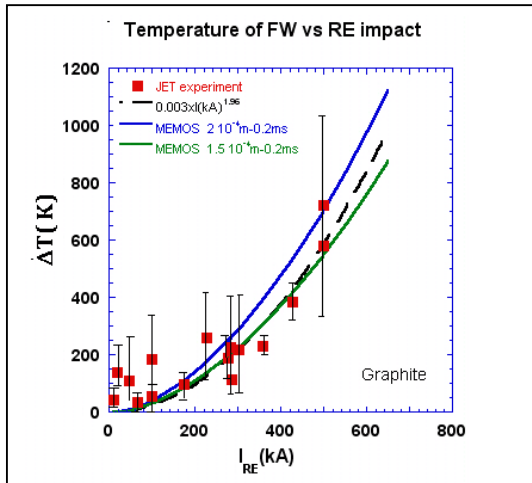


Fig. 2. Average energy increase measured on the JET FW due to RE impact as a function of the RE current - read squares; dashed curve is fit [15c]; the blue and green curves correspond the MEMOS results, shown on Fig. 1

Numerical simulations (using code ENDEP) are carried out for the sandwich target design: 2 cm CFC layer at the top of target and 1 cm Cu layer at the target bottom. It is assumed that incident electrons move along the toroidal magnetic field line ($B=3.5$ T) rotating along magnetic field lines with the Larmor frequency. Simulations are carried out for $\alpha=5$ (angle between magnetic field and wall surface), for the exponentially decaying RE distribution with $E_0=5, 8, 10$ MeV.

In the MEMOS simulations the CFC target is heated by RE beam having the Gaussian spatial profile of the energy deposition with the half-width $H_w=10$ cm and the e-beam width of 10 cm. The heat load ranged between $Q=0.5$ MJ/m² and $Q=3.5$ MJ/m² with $\tau=0.2$ ms, rectangular t-shape, and initial target temperature of 500° K are assumed. Heat conductivity coefficient is approximated by the expression: $\kappa = 4.8 + 136.4/(1 + T/300)$, which gives $\kappa = 73$ Wm/K at 0°C, and $\kappa = 42$ Wm/K at 500°C. Dependences of the maximum surface temperature versus heat load density are shown in Fig. 1 for different scenarios of the RE impact. Parallel impact of RE with $\alpha=5$ gives maximal increase of the surface temperature and maximum values of the cooling rate $(dT/dt)_-$ which is in good agreement with the experimental data of 10 - 20 K/ms. To compare in more detail results of the simulations with the data obtained at the JET experiments the dependence of surface

temperature on heat loads has to be transformed to the dependence of surface temperature on RE current. Corresponding models were developed in [9, 17] Dependence of $I(\Delta T)$ is plotted

in the Fig 2 for two cases of different resistivity corresponding to different penetration lengths mentioned above. Comparison shows a reasonable qualitative and reasonable quantitative agreement with experiment (Fig.3. [18]).

2.2 Numerical simulations of Be armour damage under runaway electrons impact

To estimate consequence of RE impact on Be FW under expected ITER transients the

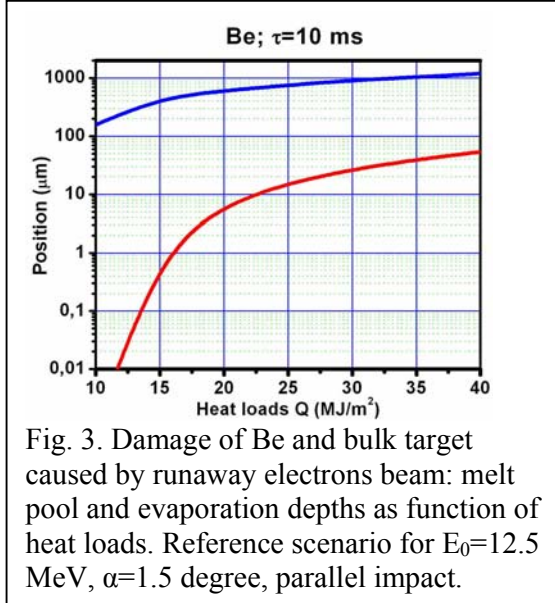


Fig. 3. Damage of Be and bulk target caused by runaway electrons beam: melt pool and evaporation depths as function of heat loads. Reference scenario for $E_0=12.5$ MeV, $\alpha=1.5$ degree, parallel impact.

following numerical simulations are carried out for the sandwich target design: 1 cm Be layer at the top of target and 1 cm Cu layer at the target bottom [7,9]. Electrons move along the toroidal magnetic field line ($B=5$ T), angle between field lines and wall surface $\alpha=1.5$ degree, and the exponentially decaying RE distribution with $E_0=12.5$ MeV is assumed. Simulations of the Be armour damage caused by the RE action are carried out for the Be bulk armour. The Be target is heated with by RAEs beam having the Gaussian spatial profile of the energy deposition with the half-width $H_w=10$ cm and the e-beam width of 5 cm. The heat load ranged between $Q=5$ MJ/m² and $Q=40$ MJ/m² with $\tau=10$ ms, rectangular t-shape and initial target temperature of 500° K are

simulated.

Results of simulations demonstrate that impacting RE heat the targets and for the most investigated here scenarios temperature significantly exceeds the melting temperature, the maximum surface temperature exceeds 2000 K at the armour surface. Due to so high temperature of the melted material huge evaporation of the Be occurs. A lot of the absorbed energy is going for evaporation. Due to this fact much less energy is spent to the melting therefore the final depth of melt pool slightly exceeds 1 mm for the heat load $Q>35$ MJ/m² (see Fig. 3). Melting threshold corresponds to $Q>5$ MJ/m². Significant evaporations starts for the heat loads $Q>12$ MJ/m² and evaporation depth reaches about 47 μm for the heat load $Q=40$ MJ/m². Melt layer exist rather long time up to 0.2 s, that is very dangerous because of melt layer instability could cause splashing. The analogous simulations carried out for the tungsten armour demonstrated melting threshold corresponding to $Q>50$ MJ/m²

3. Simulation of the tungsten cracking under plasma impact.

A dedicated series of experiments has been performed in the QSPA-Kh50 plasma accelerator [19,20] for verification of the tungsten brittle destruction model used in PEGASUS-3D code for estimation of the ITER divertor damage with ELMs of various size and time duration. The main plasma parameters are as follows: the ion energy is about 0.4 keV, maximum plasma pressure 3.2 bar (time averaged pressure during the pulse is 1.6-1.7 bar), and the plasma stream diameter 18 cm. The plasma pulse shape is triangular with pulse duration of 0.25 ms. The magnitudes of heat load Q were 0.2 MJ/m², 0.3 MJ/m², 0.45 MJ/m² (which did not cause melting) and 0.75 MJ/m² (above the melting threshold). The targets were exposed to perpendicular plasma stream.

X-ray diffraction (XRD) has been used to study the micro-structural evolution of exposed W targets. 9-29 scans were performed using a monochromatic K_α line of Cu anode radiation.

The analysis of diffraction peaks intensity, profiles, and the angular positions was applied to evaluate the macro-strain and the lattice parameters. The lattice parameter in a stress-free state $a_0 \approx (0.31640-0.31644)$ nm is close to the reference value (0.3165 nm). This is indication of the negligible number of point defects (vacancy) in the tungsten lattice of prepared targets. Residual stress at the surface of tungsten target of ITER grade has been measured after 1-5-10 shots with energy depositions of 0.2 MJ/m², 0.3 MJ/m², 0.45 MJ/m² and 0.75 MJ/m². Analysis of these measurements complemented with analytical solution for stress dependence on the coordinate perpendicular to the target surface allow explaining the physics of cracking and the reasons for the cracks pattern stabilisation, predicted in [21]. Results of the performed experiments are shown in Tables 1-3.

Cracking of the tungsten sample heated with short powerful plasma shots is due to the tensile stress which have maximum at the surface and decrease inside the target. This tensile stress arises close to the heated surface due fast re-solidification of melt if the surface melts under the plasma shot and due to the tungsten plastic deformations if it does not. The tensile stress arises in the target in course of cooling down after shot due to the plastic deformation. When the tensile stress exceeds the tensile strength value, cracks arise at the sample surface. The tensile stress at the surface under action of plasma shot of 0.3 MJ/m², being the threshold value for start of tungsten cracking, is measured as 300-380 MPa. Analytical estimations performed allow predicting that the threshold for tungsten cracking measured under action of 5-10 shots is not universal value. For larger number of shots the threshold value should decrease. A rough analytical consideration gives the value of $Q \geq 0.1$ MJ/m² for true tungsten cracking threshold for the shots of 0.25 ms time duration.

The mean crack width grows with number of shots because the time duration for plastic deformation during one shot is not enough for total relaxation of the compressive stress during heating of sample. Hence, the deformation grows with repetitive shots till the ratio of the mean crack width to the mean crack mesh size equals the linear expansion of tungsten at the maximum surface temperature. After this the compressive stress does not arise during heating, then the plastic deformation stops and, as a consequence, the cracks width and depth stabilized.

Table 1. Residual stress in MPa measured at the sample surface after 1, 5 and 10 shots (the number of shots is indicated in the second line).

T, °C Q, MJ/m ²	200			400		600	
	1	5	10	1	5	1	5
0.75	386	362	183	294	268	303	195
0.45	314	240	200	230	240	230	240
0.2	160	120		180	160	149	160

Table 2. Mean crack width in μm for large cracks of $\sim 200-300\mu\text{m}$ mean crack depth and ~ 1 mm mean crack mesh size.

T, °C	200			400		600	
No of pulses	1	5	10	1	5	1	5
0.75 MJ/m ²	X	2-4	4-8	X	X	X	X
0.45 MJ/m ²	X	0,5-1,5	1-3	X	X	X	X
0.2 MJ/m ²	X	X	X	X	X	X	X

Table 3. Mean crack width in μm for shallow cracks of $\sim 5\text{-}10\mu\text{m}$ mean crack depth and $\sim 30\text{-}50\mu\text{m}$ mean crack mesh size at the target surface.

T, °C	200			400		600	
No of pulses	1	5	10	1	5	1	5
0.75 MJ/m ²	X	0.2-0.4	0.3-0.5		0.3-0.5	0.4-0.6	~1
0.45 MJ/m ²	X	X	X	X	X	X	X
0.2 MJ/m ²	X	X	X	X	X	X	X

4. Simulation of massive gas injection with tokamak code TOKES

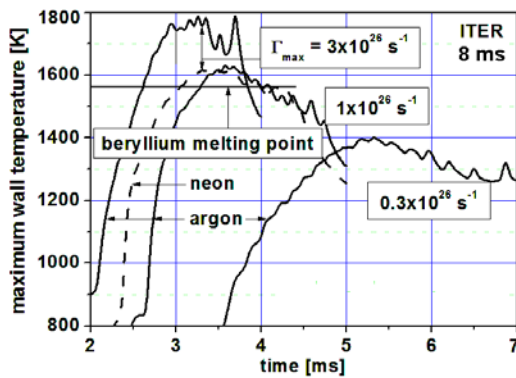


Fig. 4 Maximum Be wall temperature for ITER simulations. Γ_{max} is the maximum G-gas inflow with the pulse duration $\tau=8$ ms.

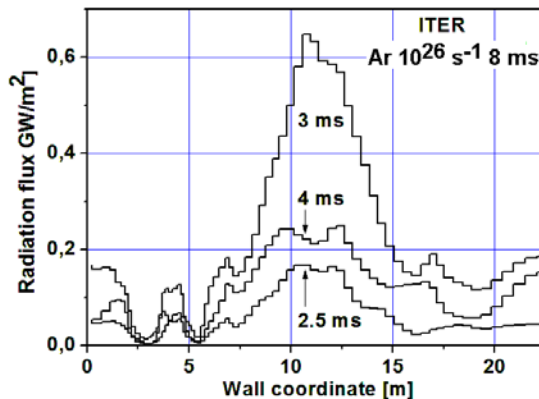


Fig. 5 Wall radiation flux for ITER for $\Gamma_{\text{max}} = 10^{26} \text{ s}^{-1}$ and $\tau=8$ ms

ionization rate resulting in deep jet penetration. In the low temperature region the Spitzer diffusion of plasma can get significant, which increases SOL thickness.

The particular features of MGI simulation are as follows. With short TQ, the magnetic field is assumed fixed and the conventional plasma transport neglected. The MGI induced MHD thermal transport bases in TOKES on a phenomenological diffusive approach. The gas

In 2009 and 2010 the modelling with the tokamak code TOKES of hot plasma, plasma contamination by impurities and radiation impacts on the wall has been focused upon mitigated disruptions anticipated in ITER [16,22]. After significant elaborations which allowed two-dimensional description of plasma cooling on millisecond time scale, TOKES addressed the actual for ITER problem of radiation wall load during the massive gas injection (MGI). The chemical elements neon and argon are added to the nomenclature of TOKES gas species. The model of 2D toroidally symmetric multi-fluid plasma includes as fast cross-diffusion as non-equilibrium expansion of plasma along magnetic field lines.

Tokamak experiments demonstrated effective ionizations of injected atoms G ($G = \text{Ne}, \text{Ar}, \text{He}$) during MGI, the following MHD activity which causes the thermal quench (TQ) within a few ms when the ionization front reached the magnetic surface of safety factor $q = 2$, and the toroidally well symmetric radiation flush. On the short time scale the ionization of G-atoms localized near the jet entry can result in plasma parameters strongly varying on poloidal coordinate y . For example the electron temperature T_e decreases drastically near the jet. This can significantly decrease the

is injected from a toroidally symmetric location, either horizontally towards the magnetic axis (for the ITER simulation) or as it is done at DIII-D. The Euler's equations for the longitudinal expansion of the fluids as well as 2D diffusion- and thermal conduction equations are numerically solved.

The newly developed TOKES MGI model is successfully compared with an MGI argon 2007 experiment on the tokamak DIII-D. Preliminary predictive simulations for ITER have been performed, with the conclusion that after the radiation flush the wall temperature can exceed the beryllium melting point in front of jet entry. The MGI for ITER is simulated in order to predict maximum temperature of beryllium first wall during the radiation flush. Initial temperature 500 K of Be wall was assumed. For MGI in ITER the TQ time of 2 ms is obtained at which the maximum wall temperature after the radiation flush exceeded Be melting point 1566 K (see Fig. 4). Fig. 5 demonstrates the calculated highly inhomogeneous distribution of radiation power over the wall.

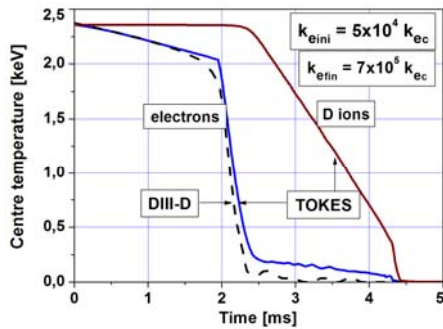


Fig. 6 Validation of TOKES by DIII-D electron temperature T_{e0} . k_{ec} is electron classical thermal conductivity.

Fig. 6 demonstrates the comparison of simulated and experimental centre temperature $T_{e0}(t)$. The fitting is achieved tuning up a few parameters which are not precisely known in the experiment but strongly influence $T_{e0}(t)$: 1) position of $q = 2$ magnetic surface which locates approximately as it can be expected in DIII-D. 2) Electron thermal conductivities of hot plasma before (k_{eini}) and after (k_{ein}) reaching the surface of $q = 2$ by the cooling front, which happened at $t = t_{q2} \approx 2$ ms after starting the gas injection.

The good fitting indicates that the simulation reproduces main processes of TQ. First consequence of core instabilities appears to be small deteriorations of toroidal symmetry and thus

slight overlapping of nested magnetic surfaces, which drastically increases electron cross-transport by thermal conductivity along entangled magnetic field lines. After start of cooling plasma periphery the instabilities can develop at many rational values of q in the core, but we assume they remain moderate until $t > t_{q2}$, due to which $k_{eini} \ll k_{ein}$ follows. The long tail of T_{e0} on Fig. 6 is due to a long electron-ion thermal energy exchange time, because centre ion temperature remains high until $t = 4$ ms (see Fig. 6).

5. Conclusions

Numerical simulations of Be and W armour damage under the runaway electron heat loads are carried out using the codes ENDEP and MEMOS validated against JET experiments. Melting thresholds for Be and W armour were determined. Numerical simulations have demonstrated that mechanism of the surface evaporation significantly (by several times) decreases the melting that is more favourable for ITER FW armour.

The tensile stress at the surface under action of plasma shot of 0.3 MJ/m^2 , being the threshold value for start of tungsten cracking, is measured as 300-380 MPa. Analytical estimations performed allow predicting that the threshold for tungsten cracking measured under action of 5-10 shots is not universal value. For larger number of shots the threshold value should decrease. Rough analytical considerations give the value of $Q \geq 0.1 \text{ MJ/m}^2$ for true tungsten cracking threshold for the shots of 0.25 ms time duration.

Preliminary 2D simulations showed that the thermal quench time of the massive gas injection shorter than 5 ms should be avoided for Be wall, which is possible choosing some optimal amount of injected gas (~10 g Ar or Ne entering the vessel prior TQ end). Successful comparison and model validation against the tokamak DIII-D is achieved. The further comparison with modern tokamaks such as JET, DIII-D and ASDEX UG should be done. The obtained results provide useful benchmarks of MGI simulations, but more work is needed for further development of the code in order to reach reliable integrated modelling including surface aspects.

Acknowledgement

This work, supported by the European Communities under the EFDA Task WP11-PWI between EURATOM and Karlsruhe Institute of Technology, was carried out within the framework of the European Fusion Development Agreement. The views and opinions expressed herein do not necessarily reflect those of the European Commission.

The views and opinions expressed herein do not necessarily reflect those of the ITER Organization.

References

- [1] ITER Physics Basis, Nucl. Fusion **39** (1999) 2137
- [2] Federici, G., et al, Plasma Phys. Control. Fusion **45** (2003) 1523
- [3] Loarte, A., et al., Physica Scripta T128 (2007) 222
- [4] Klimov, N., et al., J. Nucl. Mat. 390-391, (2009) 721
- [5] V.M. Safronov et al., J. Nucl. Mat. 386-388, (2009) 744
- [6] B. Bazylev et al. J. Nucl. Mater. 386-388 (2009) 919-921
- [7] Bazylev B. et al, 2009 ICFRM-14 Sapporo , O3 will be published in J. Nucl Mat
- [8] Bazylev B. et al J. Nucl. Mat. 390-391, (2009) 810
- [9] B Bazylev et al. Proc. 19th PSI Conference, San Diego, USA, 2010.
- [10] Bazylev B. et al, Fusion Eng. Des. 84 Iss 2 (2009) 441
- [11] Bazylev B. et al, , Physica Scripta N138 (2009), 014061
- [12] S. Pestchanyi, Fusion Eng. Des. 83 (2009) 1054
- [13] Garkusha I.E. et al, J. Nucl. Mat. 386-388, (2009) 127
- [14] I.S. Landman, G. Janeschitz, Fus. Eng. Des., 83 (2008) 1797
- [15] I.S. Landman, G. Janeschitz, J. Nucl. Mater., 390-391 (2009) 384-387,
- [16] I.S. Landman et al., Fusion Eng. Des. (2010), doi:[10.1016/j.fusengdes.2010.03.044](https://doi.org/10.1016/j.fusengdes.2010.03.044)
- [17] Yu. Igitkhanov, B Bazylev et al Proc. 19th PSI Conference, San Diego, USA, 2010.
- [18] G.Arnooux et al. Proc. 19th PSI Conference, San Diego, USA, 2010.
- [19] V A Makhraj et al, Phys. Scr. T138 (2009) 014060 (5pp)
- [20] I.E. Garkusha et al. submitted to J. Nucl. Matter
- [21] S. Pestchanyi, et al. Fus. Eng. Des (2010). doi:[10.1016/j.fusengdes.2010.05.005](https://doi.org/10.1016/j.fusengdes.2010.05.005)
- [22] I.S. Landman, S.E. Pestchanyi, Yu. Igitkhanov, R. Pitts, Two-dimensional Modelling of Disruption Mitigation by Gas Injection. To be presented at the Conference SOFT-2010, Porto, Portugal, Sep 2010.